Fermi National Accelerator Laboratory

TM-1635

Luminosity Calculation

Shao-Yuan Hsueh
Fermi National Accelerator Laboratory
P.O. Box 500
Batavia, Illinois 60510

December 1989

Operated by Universities Research Association Inc. under contract with the United States Department of Energy

Luminosity Calculation

Abstract

The luminosity of the Tevatron collider was calculated. The data used for the calculation are the flying wire transverse beam profile and the SBD bunch profile. For the 900 GeV/c mini beta runs, the calculation was compared to the CDF luminosity monitor. The ratio of the calculation and C:B0LUMP is 0.95.

by

Shao-Yuan Hsueh

I. Introduction

A program was written to calculate the luminosity of the Tevatron collider at B0 and E0. The program makes no assumption that either the longitudinal bunch shape or the transverse beam distribution is Gaussian. The variations of the beta functions and dispersion along the beam are taken into account. The program uses the flying wire data to calculate the transverse beam distribution. The longitudinal beam distribution is calculated from the SBD (sampled bunch display). The data taking is done from a console program (T116). It also initiates the calculation on the Accelerator Division VAX cluster and displays the results on the console.

II. Data and parameters

Two sets of flying wire data are used for the transverse calculation. The flying wire at C48 is used for the vertical distribution and the A17 flying wire is used for the horizontal distribution. We will use VC48 and HA17 to designate these two sets. The calculated[1] lattice functions at these two location are shown in the tables 1 and 2. Each flying wire profile consists of 192 bins over 10 mm and 7 mm for horizontal and vertical profiles respectively.

The longitudinal bunch shape is measured by the SBD which is a resistive wall current monitor. The data for each bunch has 120 bins over 18.75 ns.

The parameters used in the program are listed in table 3.

III. Unfolding SBD and flying wire data

We use ϕ and $\dot{\phi}/\omega_s$ as the longitudinal phase space coordinates. The ω_s is the synchrotron oscillation frequency. The phase trajectory is a circle in these coordinates if the bunch is much smaller than the bucket. We do not make this small-bunch approximation. Given the SBD measurement, we want to find the distribution on the ϕ and $\dot{\phi}$ plane. The SBD measures the instantaneous beam intensity which is the projection of the ϕ and $\dot{\phi}$ distribution on the ϕ axis. The measurement is done over a period Δt=18.75 ns. To change the coordinate from Δt to ϕ, we need to know the RF frequency and which bin corresponds to $\phi=0$. The RF frequency used by the program is given in table 3. To find the $\phi=0$ bin, we assume the distribution is symmetric about $\phi=0$. This is true because synchrotron oscillation about $\phi=0$ naturally symmetrizes the distribution. We use a folding algorithm that folds the distribution about every bin and compares the the two halves by calculating the χ^2. The bin that has the minimum χ^2 is the $\phi=0$ bin. The program then proceeds to symmetrize the distribution.

We will use figure 1 to illustrate the algorithm we use to find the distribution on the ϕ and $\dot{\phi}$ plane. Let N_i be the beam intensity in each ϕ-bin. We can draw the phase trajectory corresponding to each ϕ-bin. In the absence of coherent synchrotron oscillation, the particle density per unit area on the ϕ and $\dot{\phi}$ plane is constant over the annular region bounded by the phase trajectories. We get

$N_1=2*(A_{11}*P_1)$
$N_2=2*(A_{21}*P_1+A_{22}*P_2)$
$N_3=2*(A_{31}*P_1+A_{32}*P_2+A_{33}*P_3)$
.
.
.

where P_i is the particle density per unit area in the i-th annular region. The A_{ij}'s are the areas indicated in the figure. See appendix 1 on the calculation of A_{ij}. It is clear that we can solve for P_i easily. The $\Delta p/p$ distribution can be obtained by projecting the distribution on the ϕ and $\dot{\phi}$ plane on the $\dot{\phi}$ axis.

The horizontal flying wire data is described by the following convolution integral over $\Delta p/p$,

$$F(x) = \int_{-\infty}^{\infty} h_x(x - D_x \tfrac{\Delta p}{p})\, P(\tfrac{\Delta p}{p})\, d(\tfrac{\Delta p}{p}),$$

where h_x is the horizontal betatron distribution, D_x is the dispersion, and P is the $\Delta p/p$ distribution. The Fourier transform of the three distributions, F, h_x, and P, are related by

$$\tilde{F}(\omega) = \tilde{h}_x(\omega)\, \tilde{P}(D_x\omega).$$

The program calculates the Fourier transform of F(x) and $P(\Delta p/p)$, takes the ratio of the two, and does an inverse Fourier transform to get $h_x(x_\beta)$, where x_β is the x coordinate in the betatron space.

The y_β distribution is the same as the vertical flying wire distribution since the vertical dispersion is zero.

We use the same folding algorithm to find the center of the flying wire distributions. The distributions are symmetrized and smoothed.

IV. The overlapping integral

By definition luminosity is

$$L = \frac{1}{\sigma_r \tau_{rev}} \int_0^{\tau_{rev}} \int_\Omega \frac{d^2N}{d\Omega\, dt}\, d\Omega\, dt,$$

where σ_r is the total cross-section, τ_{rev} is the revolution time, and Ω is the interaction volume, $d\Omega$=dx dy ds.

For zero collision angle, we have

$$\frac{1}{\sigma_r}\frac{d^2N}{d\Omega\ dt} = (2c\beta)\rho(x,y,z,t)\bar{\rho}(x,y,z,t),$$

where $\rho(x,y,s,t)$ and $\bar{\rho}(x,y,s,t)$ are particle densities per volume of the proton and anti-proton beam respectively.

Assume that x, y, and s distributions are independent of each other, we get

$$\rho(x,y,s,t) = \int f(s-ct,\tfrac{\Delta p}{p}) g_y(y) h_x(x_\beta) d(\tfrac{\Delta p}{p})$$

$$= \int f(s-ct,\tfrac{\Delta p}{p}) g_y(\frac{y}{\sqrt{\beta_y(s)}}) h_x(\frac{x-D_x(s)\frac{\Delta p}{p}}{\sqrt{\beta_x(s)}}) \frac{1}{\sqrt{\beta_y(s)}\sqrt{\beta_x(s)}} d(\tfrac{\Delta p}{p})$$

$$\bar{\rho}(x,y,s,t) = \int \bar{f}(-s-ct,\overline{\tfrac{\Delta p}{p}}) \bar{g}_y(y) \bar{h}_x(x_\beta) d(\overline{\tfrac{\Delta p}{p}})$$

$$= \int \bar{f}(-s-ct,\overline{\tfrac{\Delta p}{p}}) \bar{g}_y(\frac{y}{\sqrt{\beta_y(-s)}}) \bar{h}_x(\frac{x-D_x(s)\overline{\frac{\Delta p}{p}}}{\sqrt{\beta_x(-s)}}) \frac{1}{\sqrt{\beta_y(-s)}\sqrt{\beta_x(-s)}} d(\overline{\tfrac{\Delta p}{p}})$$

Notice that betatron functions (β_x, β_y) and dispersion function (D_x) are functions of s. The longitudinal variations of the lattice functions along the bunches are taken into account.

We can change the variables from (x,y,s,t) to (A_x,A_y,ϕ, $\dot{\phi}$). Remember the relationships are

$$x = \sqrt{\beta_x}\, A_x$$
$$y = \sqrt{\beta_y}\, A_y$$
$$\phi = (\tfrac{\omega}{c})\,(s-ct)$$
$$\dot{\phi} = \eta\omega_{rf}\tfrac{\Delta p}{p}$$

We get

$$L = 2cf_{rev}\int dx\; dy\; ds\; dt\; \rho\,\bar{\rho}$$

$$= 2cf_{rev}\int ds\; dt\; d\left(\tfrac{\Delta p}{p}\right) d\left(\overline{\tfrac{\Delta p}{p}}\right) f\,\bar{f}\left[\frac{1}{\sqrt{\beta_y(-s)}}\int dA_y\; g_y(A_y)\,\bar{g}_y(\frac{A_y\sqrt{\beta_y(s)}}{\sqrt{\beta_y(-s)}}\right]$$
$$\left[\frac{1}{\sqrt{\beta_x(-s)}}\int dA_x\; h_x(A_x)\,\bar{h}_x(\frac{\sqrt{\beta_x(s)}\;A_x + D_x(s)\frac{\Delta p}{p} - D_x(-s)\overline{\frac{\Delta p}{p}}}{\sqrt{\beta_x(-s)}})\right],$$

where f and $\bar{f}$ are

$$f(s-ct,\tfrac{\Delta p}{p}) = (\tfrac{\omega}{c})\;\eta\omega_{rf}\; f(\phi,\dot{\phi})$$
$$\bar{f}(-s-ct,\overline{\tfrac{\Delta p}{p}}) = (\tfrac{\omega}{c})\;\eta\omega_{rf}\; \bar{f}(\bar{\phi},\bar{\dot{\phi}}).$$

The signs of longitudinal variable s are very confusing. It is easy to get the plus minus sign wrong. See figure 2 for the coordinates used.

V. Error Analysis

I estimated the numerical error using the following method. I changed the total number of bins used in the numerical integration by a factor of 4. The luminosity changed from 0.351 E30 to 0.358E30, a 1% change. I concluded that the numerical integration accuracy is $\approx$ 1%.

I also generated Gaussian profiles that approximate the actual beam profiles to check the numerical integration. For the Gaussian beam, luminosity can be calculated analytically. The results produced by the program agreed with the analytical formula to $\approx$ 1%. This small difference can be easily explained by the numerical accuracy.

We can use a elliptic bunch to test the program. The elliptic distribution (see Ohnuma, TM 1381) is described by the form

$$\rho(q,y) \propto \sqrt{y_b^2(q) - y^2},$$

where $y_b(q)$ is the boundary of the finite bunch, $y=\Delta E/\omega_{rf}$, and $q=\phi-\phi_s$.

Using the procedure outlined in the TM 1381, I found that the elliptic bunch of total bunch length of 1/3 the bucket length fitted the data. It actually fitted the bunch well except at the tails. The $\sigma(\Delta p/p)$ of the elliptic bunch can be calculated analytically. It is 1.11×10^{-4}. If we feed the elliptic distribution to the program, we get 1.14×10^{-4}. The agreement between analytic and numeric calculation is very good.

To check the transverse calculation, we generated Gaussian $\Delta p/p$ and horizontal flying wire distributions and fed them to the program. The Gaussian distributions are characterized by

σ_x(A17)	1.34 mm
$\sigma(\Delta p/p)$	1.39×10^{-4}.

The Gaussian bunch can be unfolded analytically,

$$\sigma_x^2(A17\ \textit{flying wire}) = \sigma_x^2(A17\ \textit{betatron}) + D_x^2\sigma^2(\tfrac{\Delta p}{p}).$$

From the above formula we get σ_x(A17 betatron)=0.94 mm. The program gets 0.96 mm. The agreement is very good except at the tail where the profile depends sensitively to the frequency range included in the calculation.

The proton bunch 5 of the store 1927, taken at 1/16/89/16:06 is used to illustrate the typical results of real (non-Gaussian) data. The $\Delta p/p$ distribution calculated by T116, the unfolded betatron distribution calculated by the T116, and the horizontal flying wire distribution at C48 are shown in figures 4, 5, and 6 respectively. The rms of the distributions are shown below.

σ_x(A17)	1.22 mm
$\sigma(\Delta p/p)$	1.45×10^{-4}
σ_x(unfolded betatron)	0.75 mm
σ_x(C48)	0.82 mm

If we assume the distributions are Gaussian, the σ_x after unfolding is 0.68 mm.

VI. Results

The data analyzed are tabulated in table 4. They are grouped into 6 groups, 500 GeV fixed target, 900 GeV fixed target, 900 GeV mini beta, 273 GeV fixed target, 273 GeV mini beta, and 150 GeV fixed target. Note that the C:B0LUMP for the high beta run was increased by a scale factor 1000. The luminosity for 273 GeV mini beta runs is not shown because the flying wire data is too noisy. The high frequency part of the Fourier transform of the flying wire data dominate the spectrum. The unfolded distributions at HA17 and HC48 are about a factor of 2 different.

In figure 7 we plotted the calculated luminosity vs. C:B0LUMP for the 900 GeV/c mini beta runs. The calculated luminosity is on the average .95 of C:B0LUMP.

One way to check the consistency of the lattice functions used in the program is to compare the unfolded horizontal flying wire at A17 and C48. We calculated the σ's of the unfolded distributions at the two locations for each bunch. The fractional differences are histogrammed in figure 8(a) and 8(b). The histograms peak at 0 for 900 GeV/c mini-beta and at 2.5% for fixed target data. For other energies, the differences are larger. To attempt to understand this low energy discrepancy, we plotted the ratio of the horizontal width due to dispersion and betatron motion at A17 in figure 9. The ratio varied among all energies but they didn't seem to be correlated to the differences plotted in figure 8.

Reference:

1. N. Gelfand, private communication.

TABLE I : 100% Mini Beta Lattice

	B0	E0	HA17	VC48	HC48
β_x (meter)	0.55	81.49	196.47	164.31	163.57
β_y	0.53	67.40	19.99	69.89	70.22
α_x	0.124	0.380	4.399	-1.605	-1.600
α_y	-0.049	-0.504	0.102	0.719	0.724
D_x	0.197	1.085	6.946	0.593	0.595
D_x'	-0.145	0.006	-0.126	-0.011	-0.011

TABLE II : Fixed Target Lattice

	B0	E0	HA17	VC48	HC48
β_x (meter)	72.95	71.55	76.31	105.09	104.85
β_y	73.41	73.405	38.18	27.80	27.78
α_x	-0.466	-0.470	1.572	-0.515	-0.512
α_y	0.406	0.488	-.866	-0.052	-0.043
D_x	2.433	2.481	4.964	1.964	1.963
D_x'	0.022	0.020	-0.097	0.007	0.007

TABLE III : Parameters used in the program

RF frequency	53.1 MHz
Harmonic number	1113
Radius of Tevatron	1000 meter
γ_t	18.73597

TABLE IV: Results of calculation

Time	Energy & Lattice (GeV)	B0 Luminosity (E30)	E0 Luminosity (E28)	C:B0LUMP (E30)
03/29/89 16:52	500 FT	.00061	.061255	.872
03/30/89 09:58	900 FT	.00622	.624362	.126
03/30/89 13:48		.004806	.482246	.024
04/12/89 09:53	900 Mini-beta	.91902	.968557	.948
04/12/89 12:08		.851665	.910974	.878
04/12/89 14:07		.791483	.843497	.824
04/13/89 12:00		1.36822	1.39349	1.51
04/13/89 14:02		1.31386	1.37447	1.41
05/01/89 23:51	273 FT	.001735	.17385	2.30
05/02/89 19:38		.001863	.186616	2.19
05/02/89 20:03		.001567	.157072	2.32
05/10/89 14:50	273 Mini-beta			
05/10/89 15:42				
05/10/89 16:06				
05/24/89 19:36	150 FT	.000499	.050103	.025
05/24/89 19:51		.000488	.049056	.029

Appendix I
Calculation of Aij

The constant of motion is

$$K = \dot{\phi}^2 + 2\omega_s^2 \cos\phi\,.$$

In figure 3, the area of the shaded region is

$$A = \int_{\phi_i}^{\phi_{i+1}} \sqrt{K - 2\omega_s^2 \cos\phi}\; d\phi$$
$$= \sqrt{2\omega_s} \int_{\phi_i}^{\phi_{i+1}} \sqrt{\cos(\phi_{i+2}) - \cos(\phi)}\; d\phi\,,$$

and the lower half of the shaded region is

$$B = \sqrt{2\omega_s} \int_{\phi_i}^{\phi_{i+1}} \sqrt{\cos(\phi_{i+1}) - \cos(\phi)}\; d\phi\,,$$

and upper half is, of course A-B.

Notice that the integrals are independent of RF parameters. They can be computed and stored in a file for retrieval. The program reads RF voltage each time it takes data and uses it to compute the ω_s. The area can be computed easily from the ω_s and integrals.

To calculate $\Delta p/p$ distribution, we need the similar area projected on the $\dot{\phi}$ axis. The area is

$$\int_{\dot{\phi}_i}^{\dot{\phi}_{i+1}} d\dot{\phi} \left\{ \cos^{-1}\left(\frac{K - \dot{\phi}^2}{2\omega_s^2} \right) - \pi \right\}.$$

In this case, the RF voltage cannot be factored out of the integral. The integrals are calculated for every run.

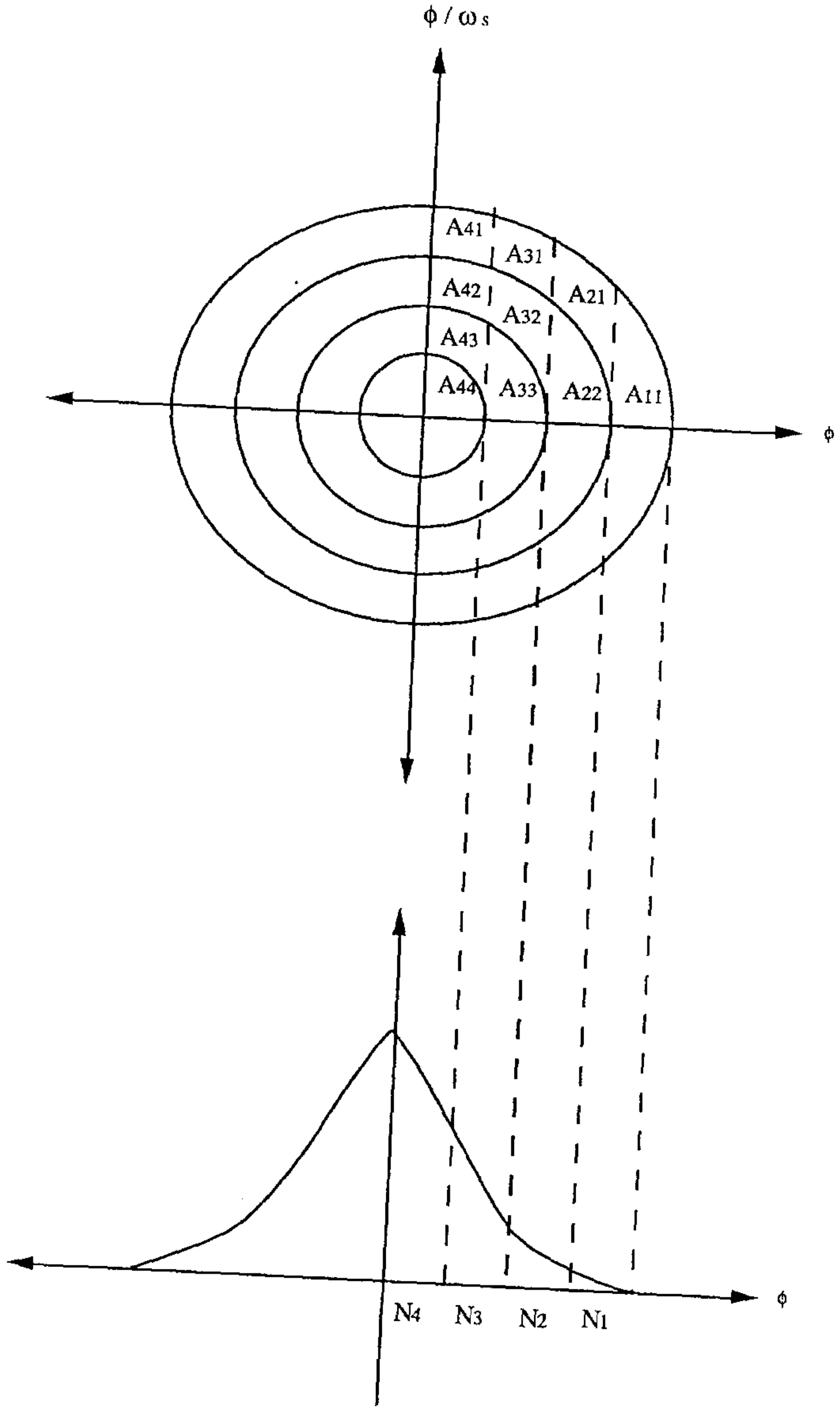

fig 1.

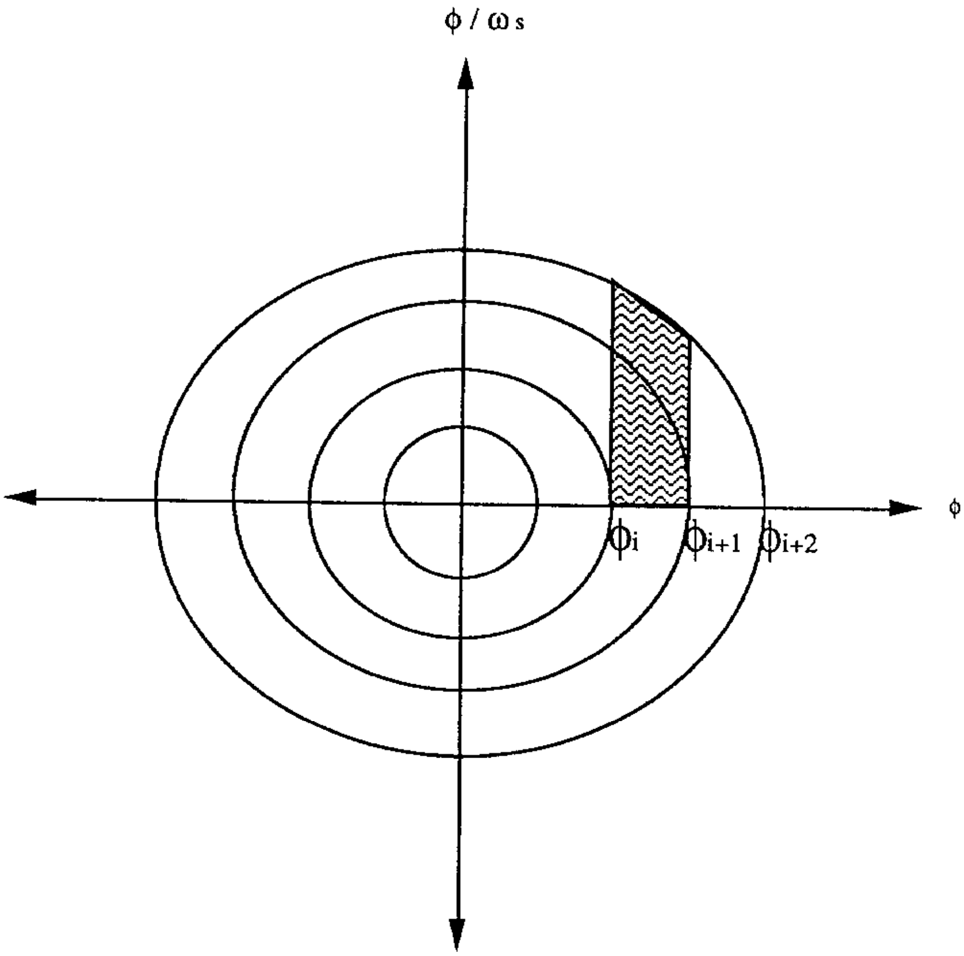

fig. 2.

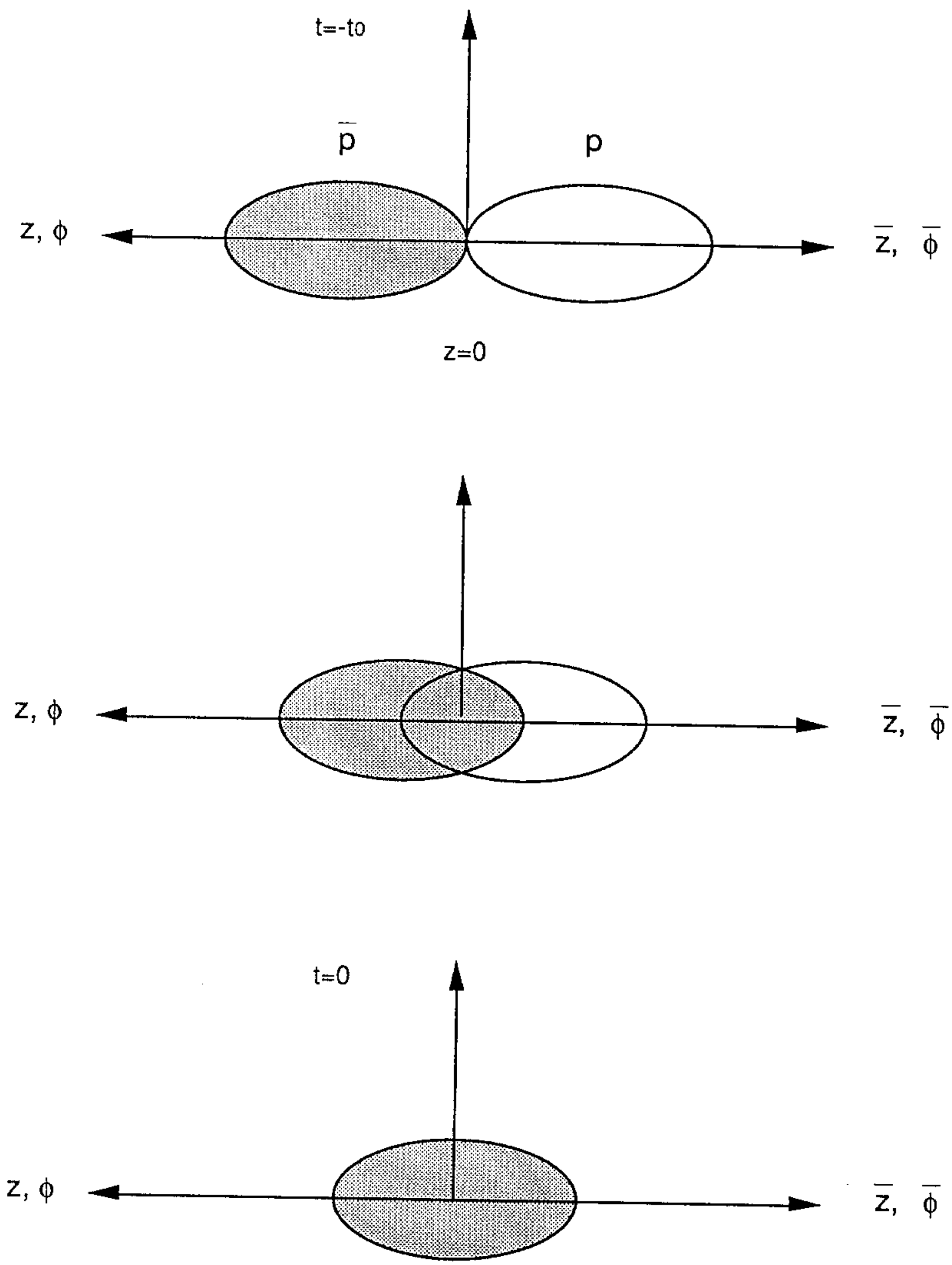
t=-to
$\bar{p}$
p
z, ϕ
$\bar{z}$, $\bar{\phi}$
z=0
z, ϕ
$\bar{z}$, $\bar{\phi}$
t=0
z, ϕ
$\bar{z}$, $\bar{\phi}$

fig 3.

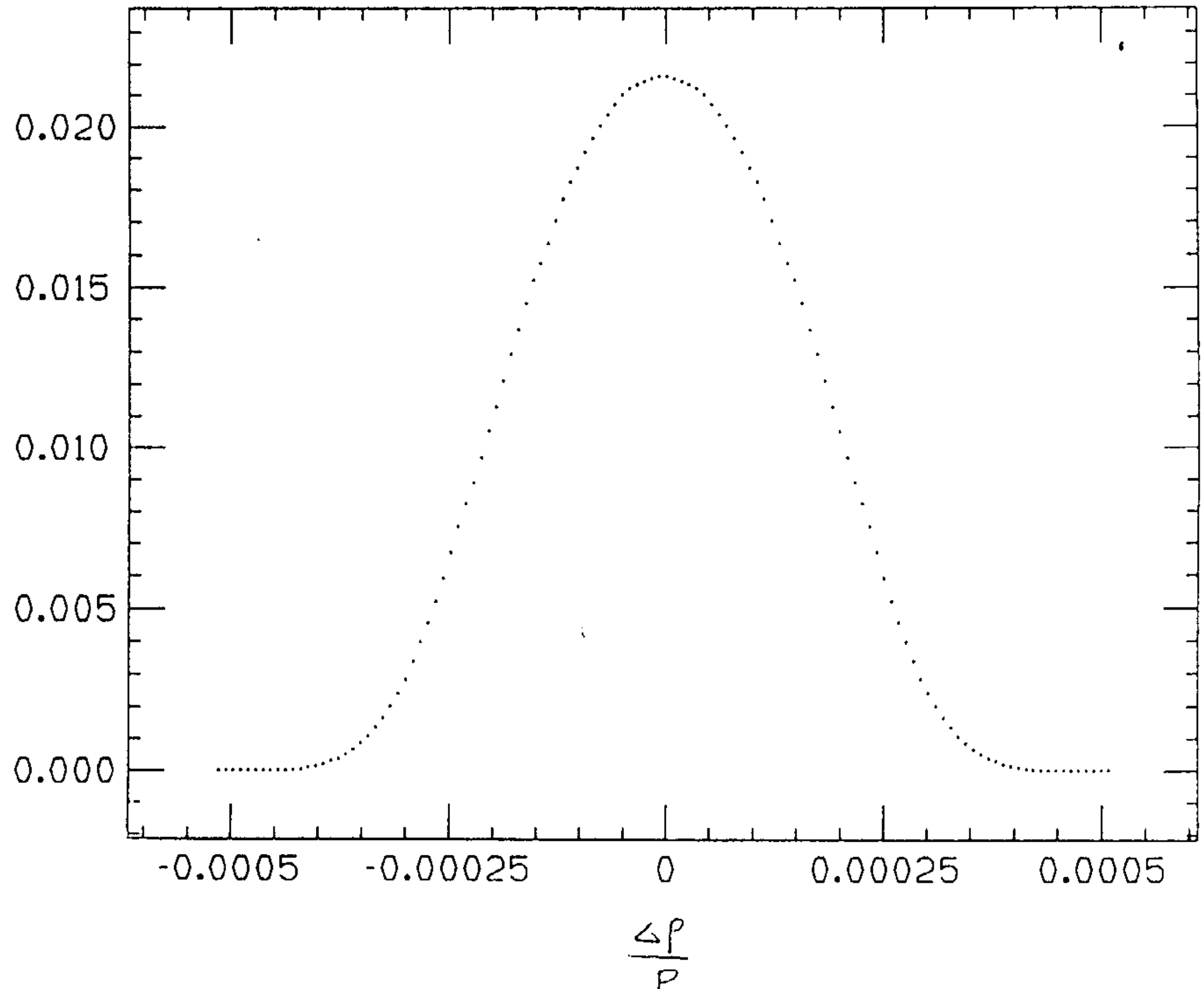
0.020
0.015
0.010
0.005
0.000
-0.0005
-0.00025
0
0.00025
0.0005
$\frac{\Delta p}{p}$

fig. 4

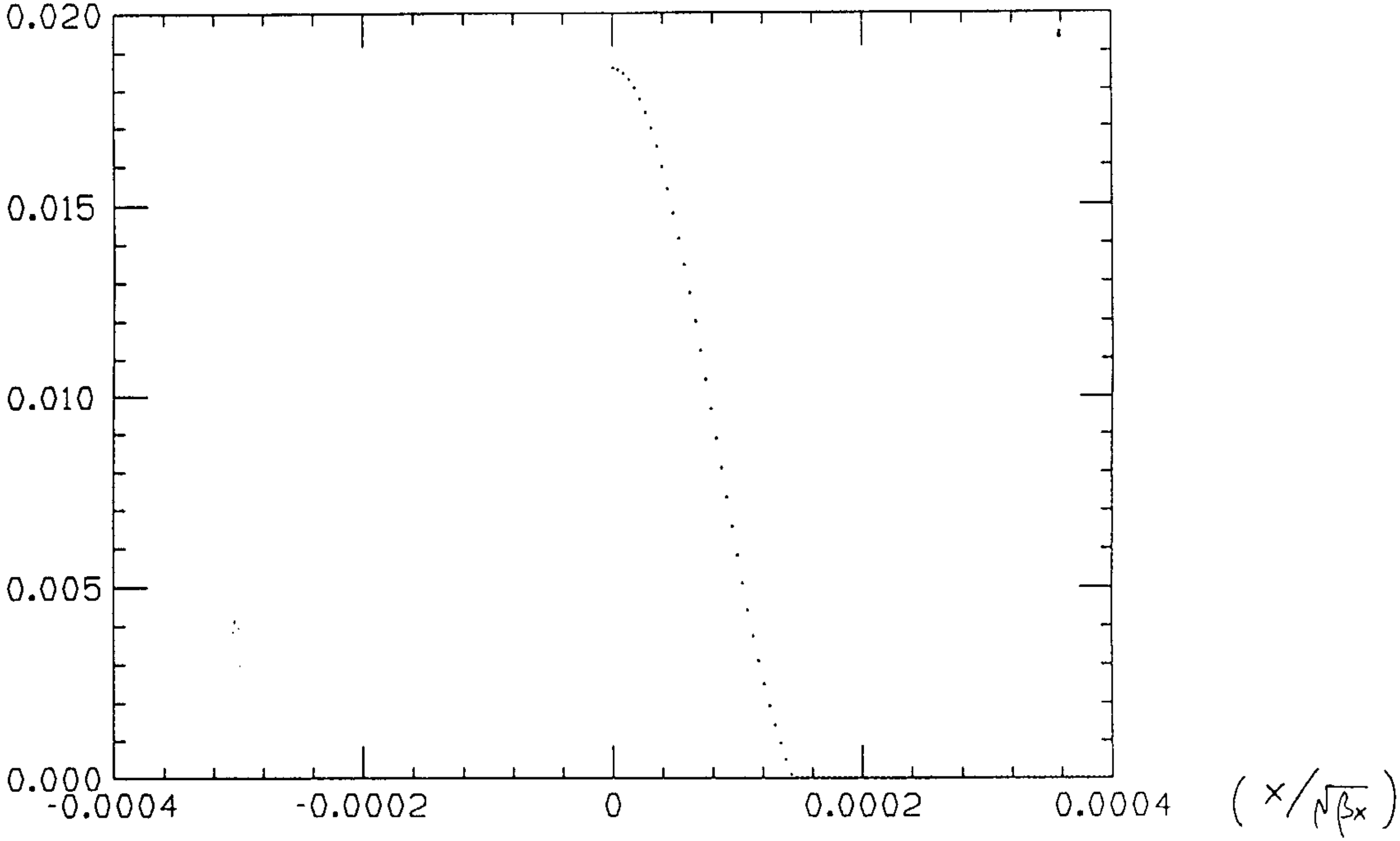

Fig 5. HA17 after unfolding

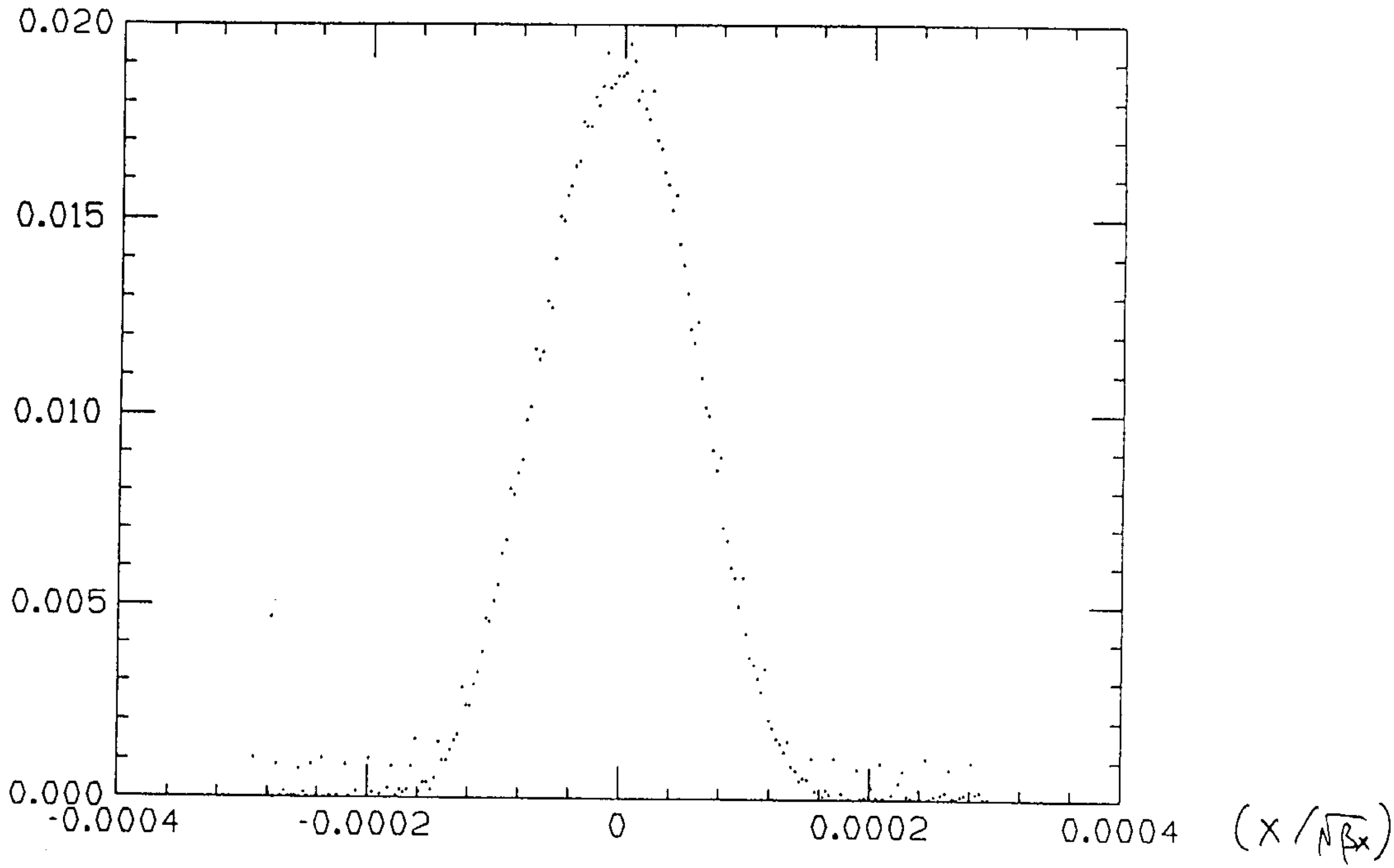

HG48 Flying Wire

Fig. 6

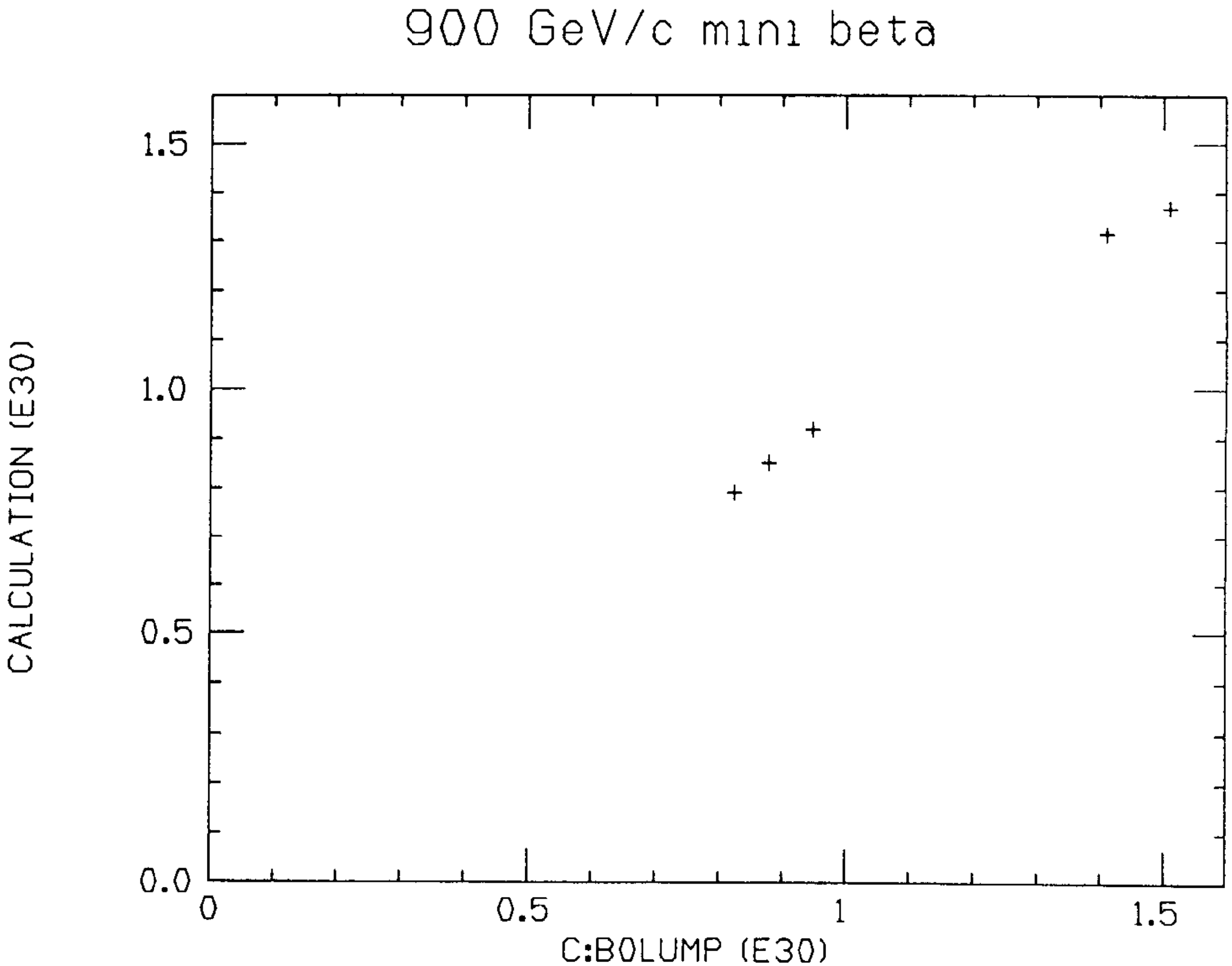
900 GeV/c mini beta
CALCULATION (E30)
1.5
1.0
0.5
0.0
0
0.5
1
1.5
C:BOLUMP (E30)

fig. 7

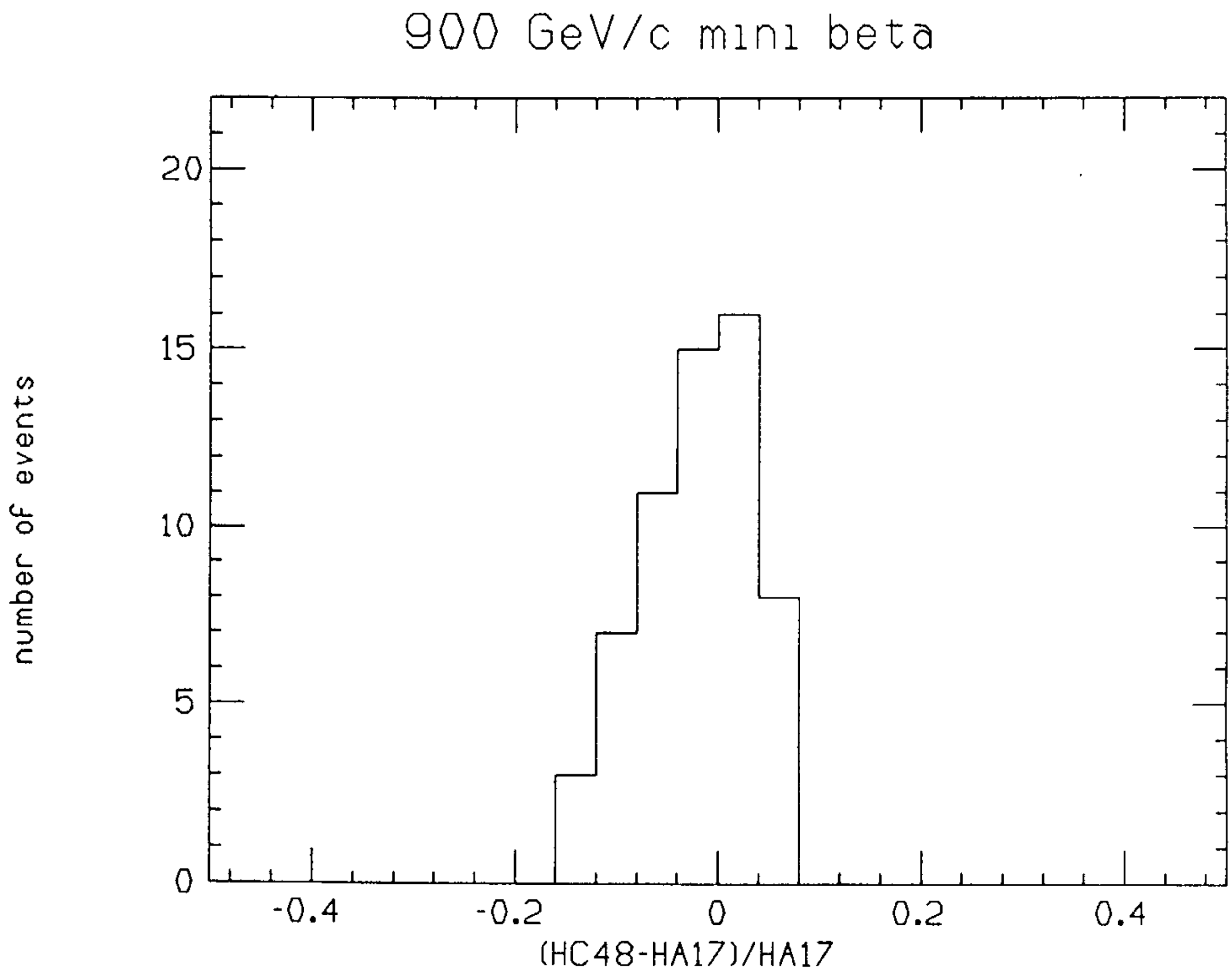
900 GeV/c mini beta
number of events
0
5
10
15
20
-0.4
-0.2
0
0.2
0.4
(HC48-HA17)/HA17

Fig 8(a)

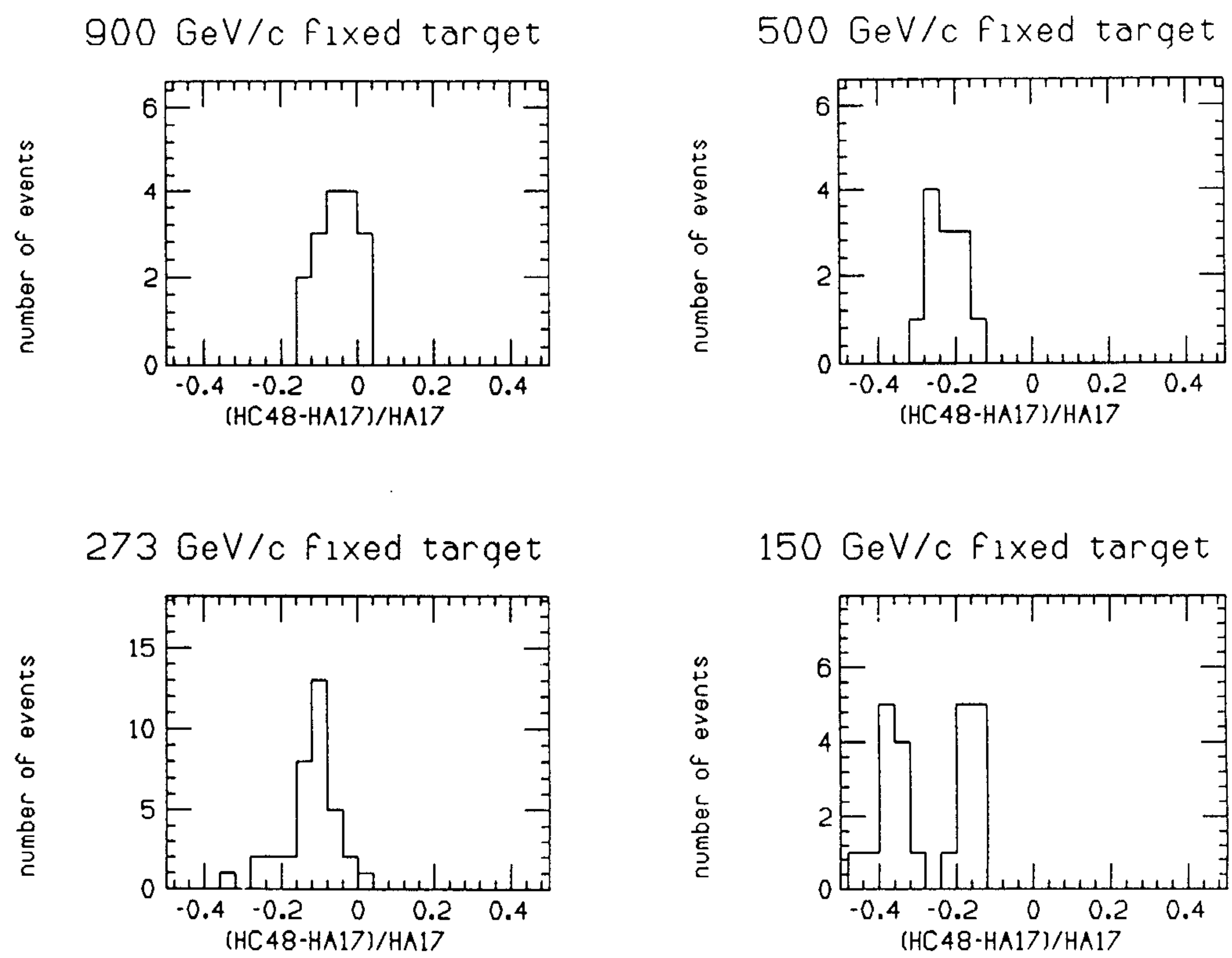
900 GeV/c fixed target
number of events
(HC48-HA17)/HA17
500 GeV/c fixed target
number of events
(HC48-HA17)/HA17
273 GeV/c fixed target
number of events
(HC48-HA17)/HA17
150 GeV/c fixed target
number of events
(HC48-HA17)/HA17

Fig. 8(b)

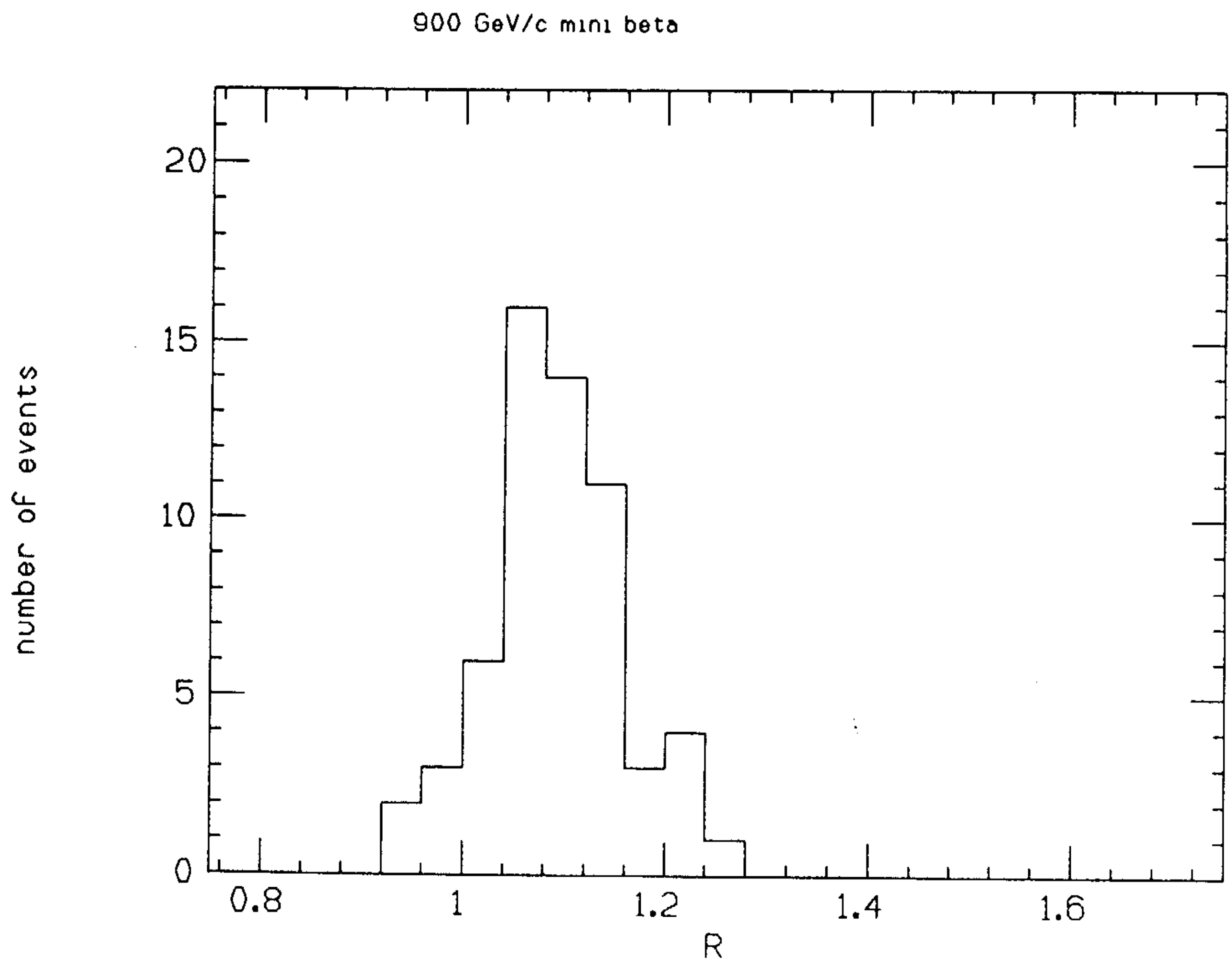

Fig. 9(a)

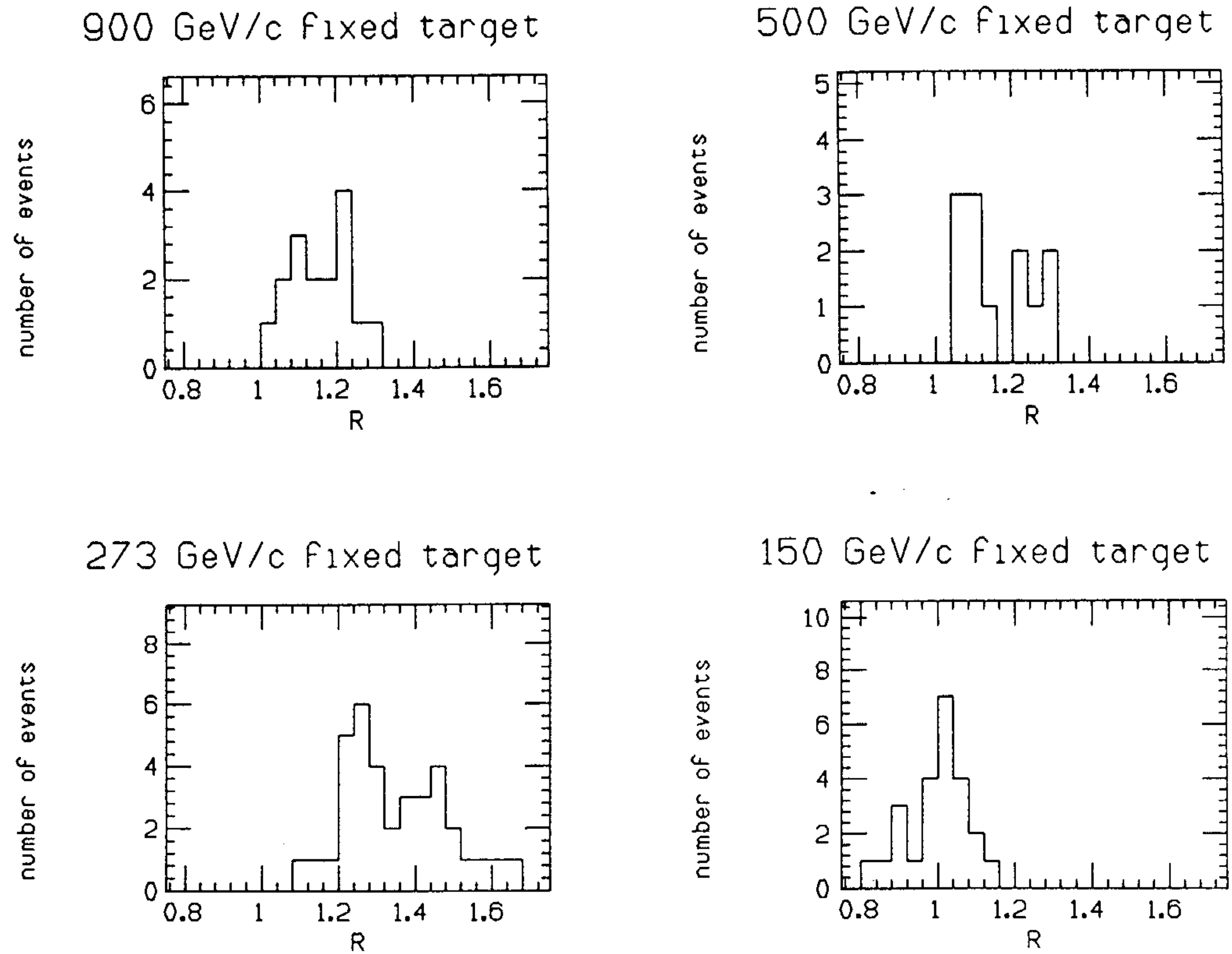
900 GeV/c fixed target
number of events
0
2
4
6
0.8
1
1.2
1.4
1.6
R
500 GeV/c fixed target
number of events
0
1
2
3
4
5
0.8
1
1.2
1.4
1.6
R
273 GeV/c fixed target
number of events
0
2
4
6
8
0.8
1
1.2
1.4
1.6
R
150 GeV/c fixed target
number of events
0
2
4
6
8
10
0.8
1
1.2
1.4
1.6
R

Fig. 9 (b)